Experiments in Fluids 6, 505–513 (1988)

Experiments in Fluids

Principles of flow field diagnostics by laser induced biacetyl phosphorescence

Liu Jian-Bang, Pan Qi, Liu Chang-Sheng, and **Shi Jie-Rong**

Institute of Mechanics, Chinese Academy of Sciences, P.O. Box 2251, Beijing, P.R. China

Abstract. A new method for measuring the density, temperature and velocity of N_2 gas flow by laser induced biacetyl phosphorescence is proposed. The characteristics of the laser induced phosphorescence of biacetyl mixed with N_2 are investigated both in static gas and in one-dimensional flow along a pipe with constant cross section. The theoretical and experimental investigations show that the temperature and density of N_2 gas flow could be measured by observing the phosphorescence lifetime and initial intensity of biacetyl triplet (^3A_u) respectively. The velocity could be measured by observing the time-of-flight of the phosphorescent gas after pulsed laser excitation. The prospect of this method is also discussed.

1 Introduction

Density and velocity measurement in gas flow by laser induced biacetyl ($CH_3COCOCH_3$ or Ac_2 for short) fluorescence or phosphorescence are new methods for flow field diagnostics. Epstein (1974) suggested visualizing streamlines and measuring the velocity by biacetyl phosphorescence. Epstein (1977) quantitatively measured the three dimensional density distribution in a transonic compressor rotor. McKenzie et al. (1979) demonstrated the measurement of relative time-dependent density fluctuation in turbulent flows by laser induced biacetyl fluorescence. Using the laser induced phosphorescence, Hiller et al. (1984) visualized the two-dimensional velocity field; Itoh et al. (1985) visualized the velocity field in a low pressure (0.5 Torr) chamber; Lowry (1987) measured the velocities on flows created by a sonic orifice and over various porous materials.

The properties of biacetyl are suitable for flow field diagnostics. It has a relatively high vapor pressure (40 Torr at room temperature) and shows no obvious condensation below 20 Torr (McKenzie et al. 1979), so that it can be easily added into a gas flow. Its high phosphorescence quantum yield (0.15: Hiller et al. 1984) makes the phosphorescence quite strong. It has a continuous broad absorption band in the visible region (3500–4700 Å); therefore many commercial lasers and spectral lamps could be used as the excitation light sources. It is flammable, nontoxic and used commonly as an additive in dairy products. The major shortcoming is that the phosphorescence can be easily quenched by O_2; consequently it must be used in an O_2-free environment.

In this paper, we shall prove that the lifetime of the biacetyl phosphorescence is a function of temperature and independent of density and concentration; the phosphorescence initial intensity is a linear function of density and insensitive to the variation of temperature; the temperature and density of N_2 flow could be measured by observing the phosphorescence lifetime and initial intensity of biacetyl mixed with N_2 respectively; the velocity could be measured by observing the time-of-flight of the phosphorescent gas after exciting with pulsed laser.

In Sect. 2.1, the phosphorescence process of biacetyl mixed with N_2 in a static cell is investigated theoretically. In Sect. 2.2, the phosphorescence intensity of one-dimensional flow in a pipe with constant cross section is analysed taking diffusion and decay effects into consideration. In Sect. 3.1, the theoretical results in static gas are examined experimentally. In Sect. 3.2, the experimental result of velocity measurement in gas flow is presented. In Sect. 4, the prospect of this method is discussed.

2 Theory

The principle of the measurements is that the phosphorescence is induced by irradiating the biacetyl with a dye laser and detected by a photomultiplier; the characteristics of the phosphorescence will be proved to be related to the temperature, density and velocity of the gas flow.

The relevant energy level diagram of biacetyl is shown in Fig. 1. The luminescent processes are as follows. After irradiation by a pulsed dye laser, the biacetyl molecules in the ground state $S_0(^1A_g)$ absorb the laser energy and transit to the singlet state $S(^1A_u)$; most of the molecules in the S state radiationlessly transit to the triplet $T(^3A_u)$ [quantum yield ~ 1, Concheaniainn and Sidebottom (1980)] under the perturbation of the spin-orbit coupling ($S \rightarrow T$ intersystem crossing), the others return to the S_0 state via either the $S \rightarrow S_0$ internal conversion or the spontaneous transition emitting fluorescence. Some of the molecules in the T state

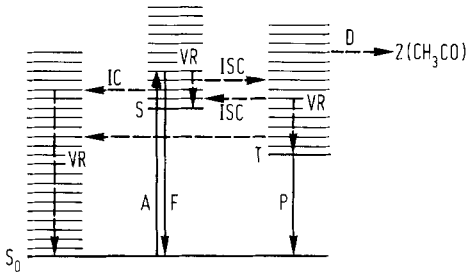

Fig. 1. Relevant energy level diagram of biacetyl; ISC: intersystem crossing; IC: internal conversion; VR: vibrational relaxation; *A*: absorption; *D*: dissociation; *F*: fluorescence; *P*: phosphorescence; S_0: ground state; *S*: singlet; *T*: triplet

return to the ground state S_0 via $T \rightarrow S_0$ intersystem crossing or the phosphorescence transition with a lifetime of 1.52 ms at room temperature; the others either transit to *S* via the $T \rightarrow S$ intersystem crossing or dissociate into $2(CH_3CO)$. It is also possible that the biacetyl molecules in the *T* state are quenched by colliding with molecules of other species, but except a few species including the O_2, the quenching rate constant is quite small.

2.1 The phosphorescence characteristics of biacetyl mixed with N_2 in a static cell

The luminescence processes can be characterized by the rate Eqs. (1) and (2) of singlet population N_S and triplet population N_T

$$\frac{dN_S}{dt} = N_{S_0} B_\lambda G W_\lambda(x,y,z,t) - N_S K_S + N_T K_{TS} \tag{1}$$

$$\frac{dN_T}{dt} = N_S K_{ST} - N_T K_T, \tag{2}$$

where

$$K_S = K_{SF} + K_{SS_0} + K_{ST} \tag{3}$$

$$K_T = K_{TP} + K_{TD} + K_{TS_0} + K_{TS}. \tag{4}$$

N_{S_0} is the population of ground state S_0, B_λ the $S_0 \rightarrow S$ absorption coefficient, $W_\lambda(x,y,z,t)$ the laser power density with wavelength λ at point (x,y,z) and time t, G the transmittance of the neutral density attenuator. K_{SF}, K_{SS_0}, K_{ST}, K_{TP}, K_{TD}, K_{TS_0} and K_{TS} are the rate constants of fluorescence, internal conversion, $S \rightarrow T$ intersystem crossing, phosphorescence, dissociation ($CH_3COCOCH_3 \rightarrow 2(CH_3CO)$), $T \rightarrow S_0$ and $T \rightarrow S$ intersystem crossing, respectively. From (1)–(4), we obtain

$$\frac{d^2 N_T}{dt^2} + (K_S + K_T)\frac{dN_T}{dt} + (K_S K_T - K_{ST} K_{TS}) N_T = K_{ST} N_{S_0} B_\lambda G W_\lambda(x,y,z,t). \tag{5}$$

The characteristic roots of relevant homogeneous equation are

$$-\gamma_T = \tfrac{1}{2}[-(K_S + K_T) + \sqrt{(K_S - K_T)^2 + 4 K_{ST} K_{TS}}] \tag{6}$$

$$-\gamma_S = \tfrac{1}{2}[-(K_S + K_T) - \sqrt{(K_S - K_T)^2 + 4 K_{ST} K_{TS}}]. \tag{7}$$

The initial conditions are

$$N_T(0) = 0, \tag{8}$$

$$N_S(0) = 0. \tag{9}$$

The rigorous solution of the Eq. (5) is

$$N_T(t) = \int_0^t \frac{e^{-\gamma_T(t-s)} - e^{-\gamma_S(t-s)}}{\gamma_S - \gamma_T} \cdot K_{ST} N_{S_0} B_\lambda G W_\lambda(x,y,z,s)\, ds \tag{10}$$

$$N_S(t) = \int_0^t \frac{(K_T - \gamma_T) e^{-\gamma_T(t-s)} - (K_T - \gamma_S) e^{-\gamma_S(t-s)}}{\gamma_S - \gamma_T} \cdot N_{S_0} B_\lambda G W_\lambda(x,y,z,s)\, ds. \tag{11}$$

For simplifying the expressions and making the comparison between the analytical and experimental results more easy the following approximations are used:

(1) We only observe the phosphorescence process, which has a time scale $t \sim 10^{-3}$ s; therefore the experimental set-up was designed to have a time resolution $\sim 10^{-5}$ s, which is far longer than the laser pulse width (1.5×10^{-8} s). Besides, the laser pulse peak is set at $t = s_M$, which is several times of the pulse width. Consequently, $W_\lambda(x,y,z,t)$ is negligible in the time periods $-\infty \rightarrow 0$ and $t \rightarrow \infty$ for the t observable in experiments. Therefore we substitute appoximately the integral limits $-\infty$ and $+\infty$ for 0 and t in Eqs. (10) and (11) $\int_0^t \rightarrow \int_{-\infty}^{+\infty}$.

Besides, the $W_\lambda(x,y,z,t)$ is approximately replaced by a δ-function centered at $t = s_M$ while the pulse energy is kept unchanged

$$W'_\lambda(x,y,z,t) \cong \left(\int_{-\infty}^{+\infty} W_\lambda(x,y,z,s)\, ds\right) \delta(t - s_M). \tag{12}$$

(2) The experimental results of van der Werf and Kommandeur (1976) show that $K_S \cong K_{ST} = 10^7 - 10^8\ s^{-1}$, $K_T \cong K_{TS}$, $K_{ST}/K_{TS} \cong 10^2 - 10^3$, therefore $K_S \cong K_{ST} \gg K_T \cong K_{TS}$, by which the γ_T and γ_S approximately are given by

$$\gamma_T \cong K_T - \frac{K_{ST} K_{TS}}{K_S - K_T} \cong K_{TP} + K_{TD} + K_{TS_0} + \frac{K_{SF} + K_{SS_0}}{K_S} K_{TS} \tag{13}$$

$$\gamma_S \cong K_S + \frac{K_{ST} K_{TS}}{K_S - K_T} \cong K_S \tag{14}$$

$$\gamma_S - \gamma_T \cong K_S. \tag{15}$$

Using these two approximations, the $N_T(t)$ and $N_S(t)$ are given by

$$N_T(t) = (e^{-\gamma_T t} - e^{-\gamma_S t}) \frac{K_{ST}}{K_S} N_{S_0} B_\lambda G \int_{-\infty}^{+\infty} W'_\lambda(x,y,z,t)\, dt \tag{16}$$

$$N_S(t) = \left(\frac{K_{ST} K_{TS}}{K_S^2} e^{-\gamma_T t} + e^{-\gamma_S t}\right) N_{S_0} B_\lambda G \int_{-\infty}^{+\infty} W'_\lambda(x,y,z,t)\, dt. \tag{17}$$

By the experimental results of van der Werf and Kommandeur (1976), $\gamma_T \sim 10^3\ s^{-1}$, $\gamma_S \sim 10^8\ s^{-1}$. Even at the beginning

of the experimental data, the processes relevant to factor $e^{-\gamma_S t}$ have already finished ($e^{-\gamma_S t} \sim 0$); therefore all the terms containing the factor $e^{-\gamma_S t}$ in (16) will be approximately neglected

$$N_T(t) = e^{-\gamma_T t} \frac{K_{ST}}{K_S} N_{S_0} B_\lambda G \int_{-\infty}^{+\infty} W'_\lambda(x, y, z, t)\, dt. \tag{18}$$

Finally, all the rate constants used above should be the statistical averages of the relevant rate constants in all vibrational levels. With all these considerations, the phosphorescence intensity received by the detector is given by

$$I_S(t) = \left(c\, h\nu\, K_{TP} \frac{K_{ST}}{K_S} NG \int_V \int_{-\infty}^{+\infty} B_\lambda W'_\lambda(x, y, z, t)\, dx\, dy\, dz\, dt \right) \cdot e^{-\gamma_T t}, \tag{19}$$

where c is a constant related to the structure of the instruments, $h\nu K_{TP}$, K_{ST} and K_S are the statistical averages of $h\nu(E_{TV}) K_{TP}(E_{TV})$, $K_{ST}(E_{SV})$ and $K_S(E_{SV})$ respectively

$$h\nu K_{TP} = \frac{\int_0^\infty \varrho(E_{TV})\, e^{-\frac{E_{TV}}{kT}} h\nu(E_{TV}) K_{TP}(E_{TV})\, dE_{TV}}{\int_0^\infty \varrho(E_{TV})\, e^{-\frac{E_{TV}}{kT}} dE_{TV}} \tag{20}$$

$$\frac{K_{ST}}{K_S} = \frac{\int_0^\infty \varrho(E_{SV})\, e^{-\frac{E_{SV}}{kT}} K_{ST}(E_{SV})\, dE_{SV}}{\int_0^\infty \varrho(E_{SV})\, e^{-\frac{E_{SV}}{kT}} K_S(E_{SV})\, dE_{SV}}. \tag{21}$$

The phosphorescence lifetime of the triplet is given by

$$\tau_T = \frac{1}{\gamma_T} = \left\{ \frac{\int_0^\infty \varrho(E_{TV})\, e^{-\frac{E_{TV}}{kT}} \left[K_{TP}(E_{TV}) + K_{TD}(E_{TV}) + K_{TS_0}(E_{TV}) + \frac{\int_0^\infty \varrho(E_{SV})\, e^{-\frac{E_{SV}}{kT}} (K_{SF}(E_{SV}) + K_{SS_0}(E_{SV}))\, dE_{SV}}{\int_0^\infty \varrho(E_{SV})\, e^{-\frac{E_{SV}}{kT}} dE_{SV}} K_{TS}(E_{TV}) \right] dE_{TV}}{\int_0^\infty \varrho(E_{TV})\, e^{-\frac{E_{TV}}{kT}} dE_{TV}} \right\}^{-1} \tag{22}$$

where V is the observed volume, $h\nu(E_{TV})$ the phosphorescence photon energy, E_{SV} and E_{TV}, $\varrho(E_{SV})$ and $\varrho(E_{TV})$ the vibrational energies of S and T states and the relevant level densities. Here the S and T states are assumed in vibrational equilibrium. The Boltzmann distribution is used because, provided the pressure is not too low, the collisional frequency between molecules is high enough (e.g., the collisional frequency at 100 Torr and room temperature is about 10^9/s), causing the vibrational relaxation rate far greater than the rate of other processes considered. In Eq. (19) the molecular number density N of biacetyl is substituted for the ground state population N_{S_0}; this is appropriate since the biacetyl lowest electronically excited state is $2 \times 10^4\,\mathrm{cm}^{-1}$ higher than the ground state (van der Werf and Kommandeur, 1976), at room temperature, $kT \cong 2 \times 10^2\,\mathrm{cm}^{-1}$, almost all of the biacetyl molecules are in the ground state, consequently $N \cong N_{S_0}$.

According to Eqs. (19) and (22), the phosphorescence intensity decays exponentially; the phosphorescence lifetime is a function of the temperature and independent of the density; the initial phosphorescence intensity determined by the pre-exponential factor in Eq. (19) is related to temperature and directly proportional to both the biacetyl number density N and the transmittance G of the attenuator. These theoretical conclusions will be examined by experimental data (Sect. 3.1) and are the basis of the temperature and density measurements.

2.2 The principle of velocity measurements

The principle of velocity measurements is shown in Fig. 2. A cylindrical lens 1 focuses the laser beam creating an approximate one-dimensional Gaussian beam. After the excitation of the laser pulse, the phosphorescent biacetyl gas, while flowing downstream, is imaged by lens 2 on a transmission grating. The phosphorescence intensity is modulated by the grating and displayed on an oscilloscope. The velocity is determined by the time-of-flight of the phosphorescent gas passing through a distance of one spatial period of the grating.

2.2.1 Equation and solution

The biacetyl triplet population $N_{TF}(x, t)$ in one-dimensional flow along a pipe with constant cross section is given by

$$\frac{\partial N_{TF}(x,t)}{\partial t} = D \frac{\partial^2 N_{TF}(x,t)}{\partial x^2} - V_x \frac{\partial N_{TF}(x,t)}{\partial x} - \gamma_T N_{TF}(x,t), \tag{23}$$

where x is the flow direction. In the right hand side of Eq. (23), the first, second and third term represent the diffusion, flow and decay processes respectively. The third term is deduced from Eq. (18). D is the mutual diffusion coefficient of N_2 and biacetyl (Present 1958)

$$D = \frac{3}{8} \frac{1}{\sqrt{2 m^* \pi}} \frac{(kT)^{3/2}}{P d_{12}} \tag{24}$$

based on a rigid elastic spheres model.

$$d_{12} = \frac{1}{2}(d_1 + d_2) \tag{25}$$

$$m^* = \frac{m_1 m_2}{m_1 + m_2}, \tag{26}$$

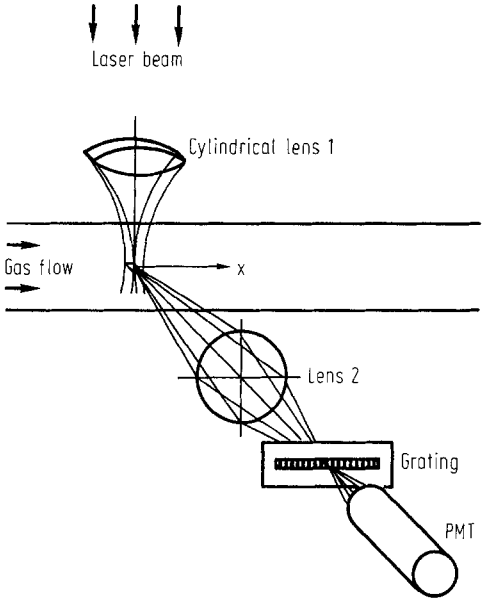

Fig. 2. Principle of velocity measurement

where d_1, d_2; m_1, m_2 are diameters and masses of N_2 and biacetyl molecules respectively. P is the pressure, V_x the component velocity in x direction. In general, D, V_x and γ_T are functions of temperature and pressure.

In Eq. (12), the time behaviour of the laser power density W_λ was approximately replaced by a δ-function; here the spatial distribution of the W_λ is assumed to be Gaussian and one-dimensional

$$W_\lambda(x, y, z, t) \cong W_\lambda(t)\, e^{-2\frac{x^2}{a_\lambda^2}}, \tag{27}$$

where a_λ is a function of λ but independent of x and t. Using Eqs. (12) and (21),

$$N_{TF}(x, 0) = A_\lambda\, e^{-2\frac{x^2}{a_\lambda^2}} \tag{28}$$

where

$$A_\lambda = \frac{K_{ST}}{K_S} N B_\lambda G \int_{-\infty}^{+\infty} W_\lambda(s)\, ds, \tag{29}$$

and N is substituted for N_{S_0} by the reason mentioned in Sect. 2.1. Equation (28) is not in contradiction with the initial condition; remembering Eq. (18), the processes with a time scale 10^{-8} sec including the absorption process were considered finished in the beginning of phosphorescence process. Equation (28) is the initial condition of Eq. (23).

In the case of one-dimensional flow along a pipe with constant cross section, D, V_x and γ_T in Eq. (23) are independent of x and t. Define a new variable

$$M(x, t) = e^{-\alpha x - \beta t} N_{TF}(x, t), \tag{30}$$

where

$$\alpha = \frac{V_x}{2D} \tag{31}$$

$$\beta = -\gamma_T - \frac{V_x^2}{4D}. \tag{32}$$

Using Eqs. (23), (28), and (30)–(32), $M(x, t)$ is given by

$$\frac{\partial M(x, t)}{\partial t} = D \frac{\partial^2 M(x, t)}{\partial x^2}, \tag{33}$$

and the initial condition is

$$M(x, 0) = e^{-\alpha x} A_\lambda\, e^{-2\frac{x^2}{a_\lambda^2}}. \tag{34}$$

The solution of Eq. (33) with initial condition (34) is given by

$$M(x, t) = \frac{A_\lambda}{\sqrt{1 + \frac{8Dt}{a_\lambda^2}}} \exp\left\{ -\frac{1}{4D}\left[\frac{x^2}{t} - \frac{\left(V_x - \frac{x}{t}\right)^2}{\frac{1}{t} + \frac{8D}{a_\lambda^2}} \right] \right\} \tag{35}$$

Using Eqs. (31), (32) and (35),

$$N_{TF}(x, t) = \frac{A_\lambda}{\sqrt{1 + \frac{8Dt}{a_\lambda^2}}} \cdot \exp\left\{ -\frac{1}{4D}\left[\frac{x^2}{t} - \frac{\left(V_x - \frac{x}{t}\right)^2}{\frac{1}{t} + \frac{8D}{a_\lambda^2}} \right] + \frac{V_x}{2D} x - \left(\gamma_T + \frac{V_x^2}{4D}\right) t \right\}. \tag{36}$$

The numerical results of $N_{TF}(x, t)$ in Fig. 3 a show obvious diffusion, flow and decay effects. Figure 3 b and c show the numerical results of $N_{TF}(x, t)$ without diffusion effect ($D = 0$) and without flow and decay effects ($V_x = 0$, $\gamma_T = 0$) respectively.

2.2.2 Relation between the phosphorescence intensity of a gas flow and a static gas

In the case without grating, the phosphorescence intensity received by the PMT from the gas flow is given by

$$I_F(t) = c\, h\, \nu\, K_{TP} \int_{-\infty}^{+\infty} N_{TF}(x, t)\, dx, \tag{37}$$

where the integral limits $-\infty$ and $+\infty$ are substituted for the dimension of observed volume. It is appropriate provided the dimension of the observed volume is far greater than that of the laser beam waist. Using the triplet population in a gas flow in Eq. (36):

$$I_F(t) = c\, h\, \nu\, K_{TP} \sqrt{\frac{\pi}{2}}\, A_\lambda\, a_\lambda\, e^{-\gamma_T t}. \tag{38}$$

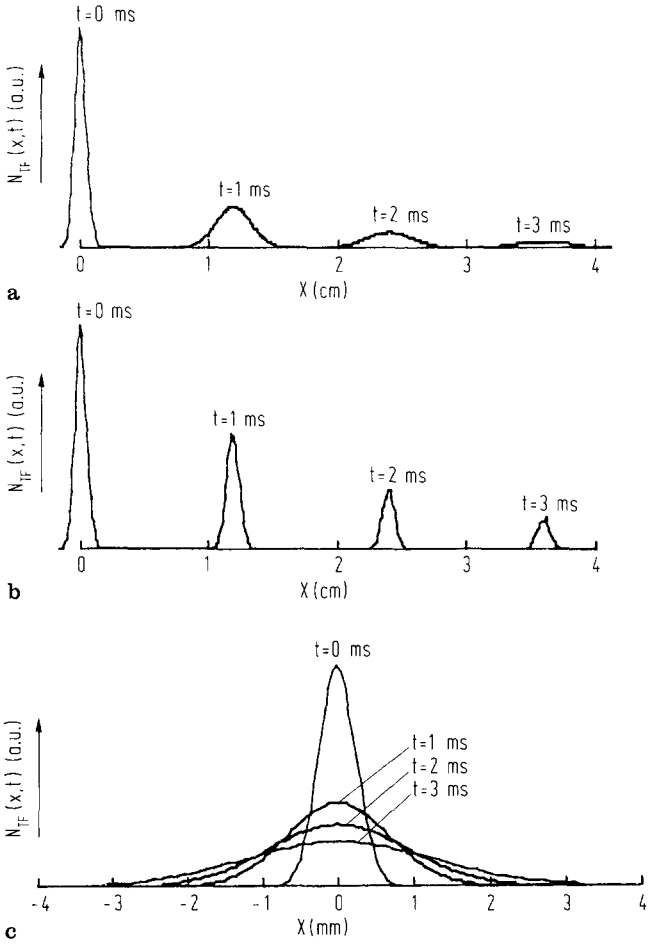

Fig. 3 a–c. The triplet population distribution $N_{TF}(x,t)$ in one dimensional flow along a pipe with constant cross section; $\lambda = 4350$ Å, $a_\lambda = 1$ mm, $P(N_2 + Ac_2) = 10$ Torr, $T = 300$ °K; **a** $N_{TF}(x,t)$ at different times; $V_x = 12$ m/s, $D = 7.9 \times 10^{-4}$ m^2/s, $\gamma_T = 667$ s^{-1}; **b** $N_{TF}(x,t)$ without diffusion effect; $V_x = 12$ m/s, $\gamma_T = 667$ s^{-1}, $D = 0$; **c** $N_{TF}(x,t)$ without flow and decay effects; $V_x = 0$, $\gamma_T = 0$, $D = 7.9 \times 10^{-4}$ m^2/s

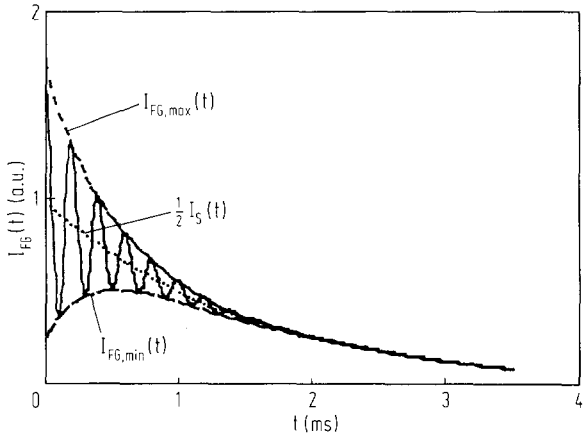

Fig. 4. An example of the phosphorescence intensity modulated by a grating with a sinusoidal density distribution; $\lambda = 4350$ Å, $f = 1/4$ mm^{-1}, $m = 1$, $a_\lambda = 1$ mm, $V_x = 20$ m/s, $T = 300$ °K, $P(N_2 + Ac_2) = 10$ Torr

On the other hand, in the case of a static gas, using Eq. (19) and the assumption of Gaussian beam (27), the phosphorescence intensity received by the PMT from static gas is given by

$$I_S(t) = c\,h\,\nu\,K_{TP}\frac{K_{ST}}{K_S} NG\left(\int_{-\infty}^{+\infty}\int_{-\infty}^{+\infty} B_\lambda W_\lambda(t)\, e^{-2\frac{x^2}{a_\lambda^2}}\, dx\, dt\right) e^{-\gamma_T t} \tag{39}$$

where the $-\infty$ and $+\infty$ are again substituted for the dimension of the observed volume. The final results of Eqs. (38) and (39) show

$$I_F(t) = I_S(t), \tag{40}$$

which implies that the phosphorescence intensity received from a gas flow is the same as that received from a static gas, provided the dimension of the observed volume is far greater than that of the laser beam waist. Therefore all the conclusions about the phosphorescence intensity drawn in the case of a static gas are applied in the case of gas flow.

2.2.3 The effects of the grating on the phosphorescence intensity

Suppose a grating with a sinusoidal density distribution (Goodman 1968) is used, the transmittance of which is given by

$$T = \frac{1}{2} + \frac{m}{2}\cos(2\pi f x) \tag{41}$$

where f is the grating frequency, m is the peak to peak change of amplitude transmittance. The spatial period of this grating is given by

$$x_0 = \frac{1}{f}. \tag{42}$$

The phosphorescence intensity after passing through the grating is given by

$$I_{FG}(t) = c\,h\,\nu\,K_{TP}\int_{-\infty}^{+\infty} N_{TF}(x,t)\,T(x)\,dx \tag{43}$$

$$= \frac{1}{2}\sqrt{\frac{\pi}{2}}\, c\,h\,\nu\,K_{TP}\,A_\lambda\,a_\lambda \cdot e^{-\gamma_T t}\left[1 + m\exp\left\{-\frac{a_\lambda^2}{8}\left(1+\frac{8Dt}{a_\lambda^2}\right)(2\pi f)^2\right\} \cdot \cos(2\pi f V_x t)\right]. \tag{44}$$

The $I_{FG}(t)$ is a modulated decay curve, an example of which is shown in Fig. 4. The period of modulation decided by the factor $\cos(2\pi f V_x t)$ in Eq. (44) is given by

$$t_0 = \frac{1}{V_x f}. \tag{45}$$

Using Eq. (42)

$$V_x = \frac{x_0}{t_0}. \tag{46}$$

It indicates that the velocity is given by the spatial period of the grating divided by the period of modulation of the phosphorescence intensity after passing through the grating. Both x_0 and t_0 could be easily and precisely determined from experimental data. Define

$$I_{FG,\mathrm{Max}}(t) = c\,h\,\nu\,K_{TP}\,\frac{1}{2}\sqrt{\frac{\pi}{2}}\,A_\lambda a_\lambda \cdot e^{-\gamma_T t}\left[1 + m\exp\left\{-\frac{a_\lambda^2\pi^2}{2x_0^2}\left(1+\frac{8Dt}{a_\lambda^2}\right)\right\}\right] \quad (47)$$

$$I_{FG,\mathrm{Min}}(t) = c\,h\,\nu\,K_{TP}\,\frac{1}{2}\sqrt{\frac{\pi}{2}}\,A_\lambda a_\lambda \cdot e^{-\gamma_T t}\left[1 - m\exp\left\{-\frac{a_\lambda^2\pi^2}{2x_0^2}\left(1+\frac{8Dt}{a_\lambda^2}\right)\right\}\right], \quad (48)$$

they could be determined by experimental data (Fig. 4). In consequence $I_S(t)$ could be determined by

$$I_S(t) = I_{FG,\mathrm{Max}}(t) + I_{FG,\mathrm{Min}}(t). \quad (49)$$

Using Eqs. (46), (49), (40) and the conclusion in Sect. 2.1, the velocity, temperature and density could be simultaneously determined by the same $I_{FG}(t)$ signal, although the modulation by a grating is not necessary for temperature and density measurements. The detection limit is determined by SNR = 3. For this flow field diagnostics method by modulated phosphorescence intensity, it is given by

$$I_{FG,\mathrm{Max}}(t) - I_{FG,\mathrm{Min}}(t) \geqq 3\,I_N, \quad (50)$$

where I_N is the intensity of noise. Using Eq. (47) and (48), inequality (50) becomes

$$-\gamma_T t - \frac{a_\lambda^2\pi^2}{2x_0^2}(1+8Dt) \geqq \ln\left(\frac{3\,I_N}{c\,h\,\nu\,K_{TP}\,A_\lambda\,m\,a_\lambda}\sqrt{\frac{2}{\pi}}\right). \quad (51)$$

Remembering that the γ_T is a function of temperature, Eqs. (22) and (52), the D is a function of temperature and pressure, Eq. (24), the inequality (51) gives the regions of T, P and t, in which the suggested method is applied.

3 Experimental set-up and results

3.1 The phosphorescence characteristics of biacetyl mixed with N_2 in a static cell

The experimental set-up is shown in Fig. 5. A N_2 laser pumped dye laser (pulse energy 0.5 mJ, pulse width 1.5×10^{-8} s and repetition rate 3 Hz) was chosen as the excitation light source. The excitation wavelength was 4350 Å (laser dye: Coumarin 120) for most of the experiments. After evacuating to 10^{-4} Torr, the glass sample cell was filled with a mixture of N_2 (purity 99.999%) and biacetyl vapor, which was prepared by evaporating the liquid biacetyl at room temperature after degassing. The sample cell was located in a thermostat and a neutral density attenuator was placed in front of the sample cell to slow down the triplet-triplet annihilation process in order to avoid its influence. The transmittance of the attenuator chosen should ensure the phosphorescence decay curve to be single-exponential in a period of twice the lifetime. For monitoring the variation of the laser output, a reference cell was used. The output optical signals of both the sample and reference cells were filtered with an interference filter (4800 Å long pass) for rejecting the laser and fluorescence signals, detected by the PMT and then either recorded by the oscilloscope camera or processed by a boxcar and recorded by X-Y plotter.

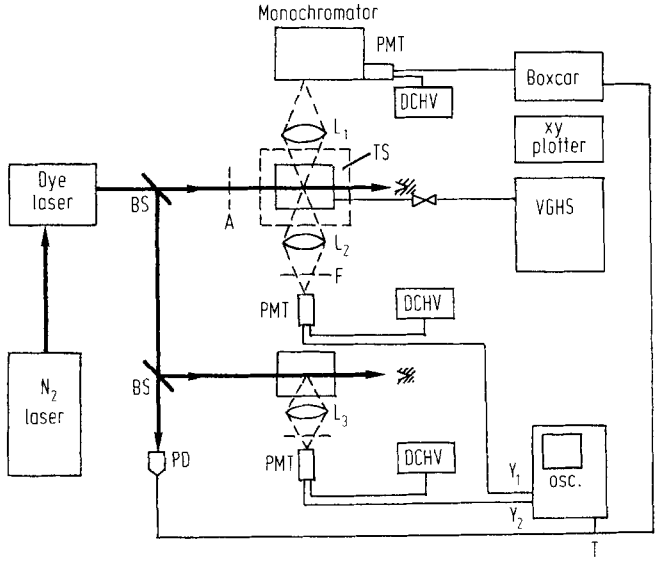

Fig. 5. Experimental set-up for investigating the phosphorescence characteristics of biacetyl mixed with N_2 in a static cell; BS: beam splitter; PD: photodiode; A: attenuator; L: lens; F: filter; PMT: photomultiplier tube; TS: thermostat; DCHV: high voltage power supply; VGHS: vacuum and gas handling system

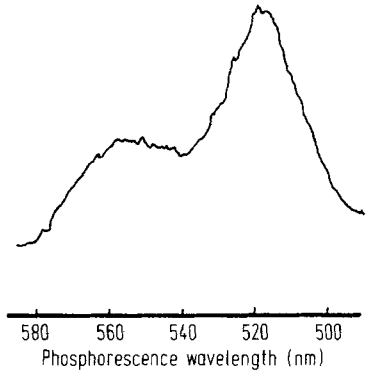

Fig. 6. Laser induced biacetyl phosphorescence spectrum; excitation wavelength: 425 nm

The laser induced biacetyl phosphorescence spectrum, as shown in Fig. 6, is a broad band between 4900–5800 Å, the highest peak is near 5175 Å, which agrees with the Okabe's experimental results (Okabe & Noyes 1957). The laser induced phosphorescence intensity decays exponentially at

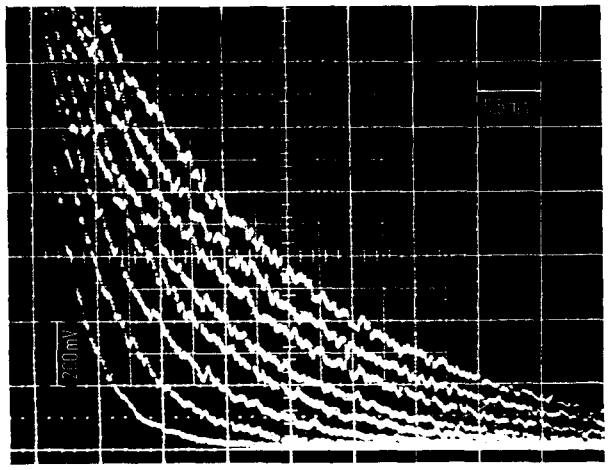

Fig. 7. Decay curves of biacetyl phosphorescence at several temperatures; density ($N_2 + Ac_2$): 1.2×10^{-2} mol/l; biacetyl density: 6.0×10^{-4} mol/l; temperature (from top to bottom): 25, 45, 60, 72, 80, 89, 101 and 108 °C, respectively; scale of abscissa: 0.5 ms/div

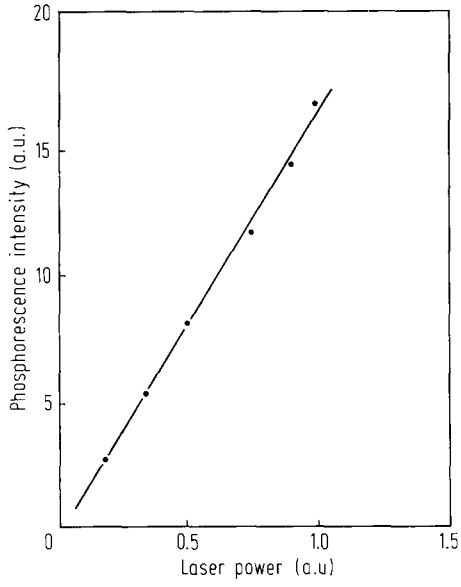

Fig. 8. Dependence of biacetyl phosphorescence intensity on incident laser power

several temperatures as shown in Fig. 7. Varying the incident laser power by using a series of neutral density attenuators with different calibrated transmittance, the phosphorescence intensity varies linearly with incident laser power (Fig. 8). It implies that the laser intensity used did not reach the saturation value, therefore the saturation effect can be neglected. The density and temperature dependences of initial phosphorescence intensity were carefully investigated at different concentrations and densities. The initial phosphorescence intensity means the phosphorescence intensity at $t = 0$. But at this moment, the laser radiation, fluorescence and electric noise are very strong causing a poor signal-to-noise ratio. Besides, as mentioned in Sect. 2.1, there is an undesired signal related to the factor $e^{-\gamma s t}$ in Eq. (16). But all of these disappear 20 μs later, so that the values of the initial phosphorescence intensities were determined by extrapolating the experimental curves after $t = 20$ μs to $t = 0$. The introduced error is negligible since the decay curves are single exponential and the extrapolation point is very close to $t = 0$ (20 μs is only 1% of the lifetime). The density dependence of initial phosphorescence intensity is shown in Fig. 9, in which the ordinate is normalized to the largest initial phosphorescence intensity of each run, and the abscissa is normalized to the highest density of each run. The experimental values and their error bars were calculated from the experimental results with 14 sets of different parameters, which cover the following ranges: temperature 26–80 °C, density $7.6 \times 10^{-4} - 0.041$ mol/l, biacetyl density $1.2 \times 10^{-6} - 2.3 \times 10^{-3}$ mol/l and biacetyl concentration 0.001 – 0.06. Figure 9 shows that the initial phosphorescence intensity is a linear function of density, which agrees with Eq. (19).

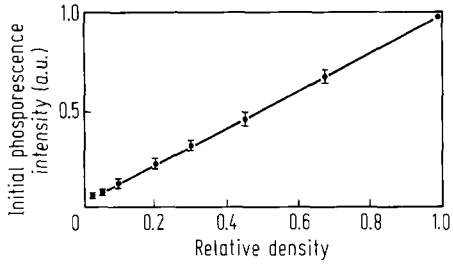

Fig. 9. Dependence of initial biacetyl phosphorescence intensity on density

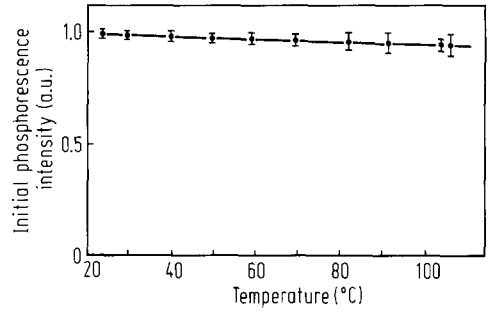

Fig. 10. Dependence of initial biacetyl phosphorescence intensity on temperature

Figure 10 shows that the initial phosphorescence intensity is a function of temperature as predicted by Eq. (19), but it is insensitive to the variation of temperature, only a linear decrease of 5% was observed in the temperature region of 20–100 °C. It implies that the initial phosphorescence is approximately independent of the temperature. Concheanainn and Sidebottom (1980) reported similar experimental results. This experimental result is favourable to the density measurement. Figure 11 shows that in the temperature region between 18 and 19 °C, the phosphorescence decay curves are purely single exponential as predicted by Eq. (19), but above 90 °C its logarithm departs from a straight line. Figure 12

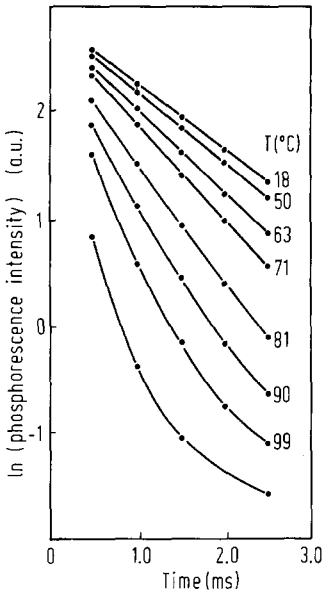

Fig. 11. Logarithmic decay of biacetyl phosphorescence

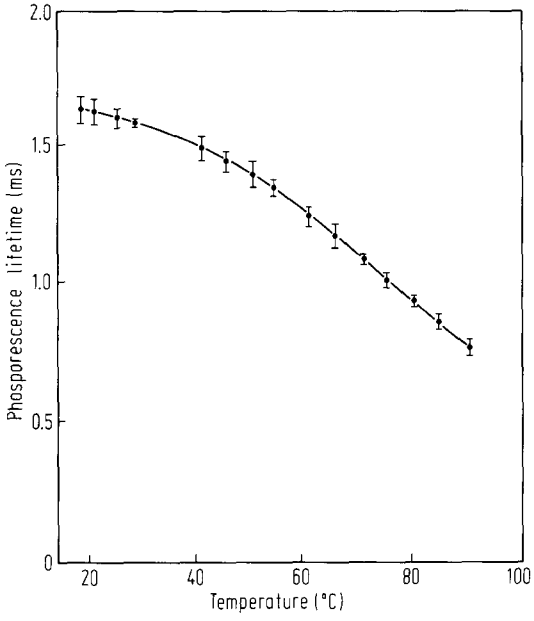

Fig. 12. Temperature dependence of biacetyl triplet (^3A_u) lifetime

shows the absolute temperature T dependence of the phosphorescence lifetime τ_T, the empirical formula of which is

$$\tau_T = \left(586 + 3.40 \times 10^8 \, e^{-\frac{4.76 \times 10^3}{T}}\right)^{-1} \text{ sec.} \quad (52)$$

This empirical formula was obtained by fitting the expression with the experimental results with 14 sets of different parameters, which cover the following ranges: temperature 18–19 °C, density $4.4 \times 10^{-3} - 0.033$ mol/l, biacetyl density $4.0 \times 10^{-5} - 2.3 \times 10^{-3}$ mol/l and biacetyl concentration 0.001–0.30. Figure 12 shows that the phosphorescence lifetime is a function of temperature but independent of density and concentration, which agrees with Eq. (22) and the experimental results reported by Concheanainn and Sidebottom (1980) and Okabe and Noyes (1957).

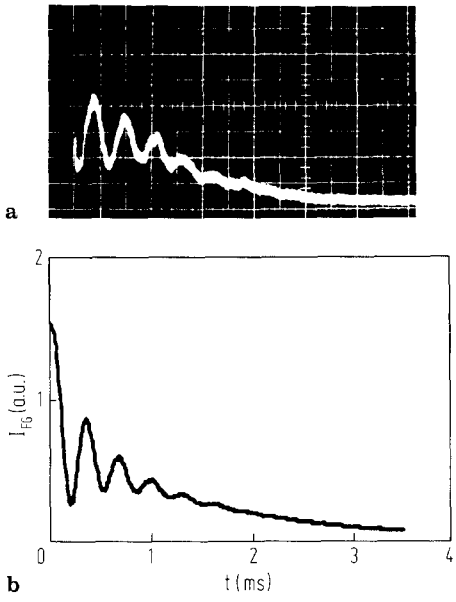

Fig. 13 a and b. Phosphorescence intensity modulated by a grating with a square wave form density distribution; **a** experimental result; scale of abscissa: 0.5 ms/div; **b** computed result; $\lambda = 4350$ Å, $a_\lambda = 1$ mm, $P(N_2 + Ac_2) = 10$ Torr, $T = 300$ °K, $V_x = 12.5$ m/s, $f = 1/4$ mm^{-1}, $m = 1$

3.2 *Velocity measurement in gas flow*

The experimental arrangement was almost the same as shown in Fig. 2. A transmission grating with square wave form density distribution was used instead of one with sinusoidal density distribution. The magnification of lens 2 was one. The phosphorescence intensity modulated by such a transmission grating was computed numerically. Both the computed and experimental results are shown in Fig. 13 and agree with each other.

4 Discussion on the possibility of flow field diagnostics by laser induced biacetyl phosphorescence

(1) Temperature measurement: The temperature of N_2 gas flow could be measured by the phosphorescence lifetime of biacetyl triplet, which is a function of temperature and independent of density and concentration as shown in Fig. 12 and Eqs. (22) and (52).

(2) Density measurement: The density of N_2 gas flow could be measured by the initial phosphorescence intensity of biacetyl triplet, which is a linear function of density and insensitive to the variation of temperature. The approximate density could be directly determined by Fig. 9, in the case of

a wide temperature variation or precise measurement, the density value obtained should be corrected by Fig. 10 with the measured temperature.

(3) Velocity measurement: The velocity of N_2 gas flow could be determined by measuring the period of the grating and the period of modulation of the phosphorescence intensity by the grating. Compared with the Doppler anemometer, it avoids to a great extent the "particle lag" problem. Therefore, it might be used in flow fields with large velocity gradients, e.g., in the ultra centrifuge and turbine or at positions near a shock wave front and in boundary layers.

(4) Measurements in low density flow fields: The density, temperature and velocity measurements mentioned above are based on the detection of the biacetyl phosphorescence. Due to the high quantum yield and broad absorption band, the biacetyl phosphorescence signals are generally strong. In our experiments, it is not very difficult to detect the phosphorescence signals even at the lowest density used (7.6×10^{-4} mol/l with a biacetyl density 1.2×10^{-6} mol/l). We suppose that, if more advanced equipment is used, the suggested method could be applied to flow fields with a density lower than 5.9×10^{-4} mol/l (10 Torr at room temperature). Itoh et al. (1985) demonstrated that the flow field visualization by biacetyl phosphorescence with gas density as low as 2.9×10^{-5} mol/l (0.5 Torr at room temperature) is possible.

(5) Two-dimensional measurements: As with many other flow field diagnostic methods based on lasers, two-dimensional temperature and density measurements could be realized by focusing the laser radiation into a thin sheet with a cylindrical lens and detecting the phosphorescence with a two-dimensional detector array. With a laser beam perpendicular to the flow direction, one-velocity-component measurements in the plane containing the laser beam and the flow direction could be realized.

(6) In principle, temperature, density and velocity signals could be acquired simultaneously by one laser pulse.

(7) Limitations and shortcomings: (a) The phosphorescence lifetime measurement takes 1–2 ms, during which time, the density and temperature of the phosphorescent gas should have no observable variation. Therefore, in a flow with density and temperature changing rapidly in space, the temperature measurement can only be carried out in the area with low flow velocity. Note that this limitation dose not apply to density and velocity measurements. (b) As mentioned above, O_2 quenches the biacetyl phosphorescence rapidly; consequently the measurements should be carried out in an O_2-free environment. In practice, this can be met by evacuating the experimental section to 10^{-4} Torr and using N_2 of purity 99.999%.

5 Acknowledgements

The authors thank Prof. Wu Cheng-Kang and Prof. Xie Bo-Ming for their fruitful discussions, Mr. Xia Sheng-Jie, Mr. Bai Shuang-E and Mrs. Xia Lu-Hua for their kind assistances. The authors thank National Natural Science Foundation of China and The Third World Academy for their support.

References

Concheanainn, C. O.; Sidebottom, H. W 1980: Temperature dependence of the triplet lifetime of biacetyl in the gas phase. J. Photochem. 13, 55–66

Epstein, A. H. 1974: Fluorescence gaseous traces for three dimensional flow visualization. MIT GTL rep. no. 117

Epstein, A. H. 1977: Quantitative density visualization in a transonic compressor rotor. J. Eng. Power 99, 460–475

Goodman, J. W. 1968: Introduction to Fourier optics. New York: McGraw-Hill

Hiller, B.; Booman, R. A.; Hassa, C.; Hanson, R. K. 1984: Velocity visualization in gas flow using laser induced phosphorescence of biacetyl. Rev. Sci. Instrum. 55, 1964–1967

Itoh, F.; Kychakoff, G.; Hanson, R. K. 1985: Flow visualization in low pressure chambers using laser induced biacetyl phosphorescence. J. Vac. Sci. Technol. B3, 1600–1603

Lowry, H. S. 1987: Velocity measurements using the laser-induced phosphorescence of biacetyl. AIAA-pap. 87-1529

McKenzie, R. L.; Monson, D. J.; Exberger, R. J. 1979: Time-dependent local density measurement in unsteady flows. NASA rep. no. 791088

Okabe, H.; Noyes, W. A. Jr. 1957: The relative intensities of fluorescence and phosphorescence in biacetyl vapor. J. Am. Chem. Soc. 79, 801–806

Present, R. D. 1958: Kinetic theory of gases. New York: McGraw-Hill

van der Werf, R.; Kommandeur, J. 1976: The electronic relaxation of biacetyl in gas phase. Chem. Phys. 16, 125–150

Received March 1, 1988